6th Australasian Hydraulics and
Fluid Mechanics Conference
Adelaide, Australia, 5-9 December 1977

# The Effect of the Temporal Distribution of Rainfall on Infiltration Rate and Surface Runoff

S. J. LEES
Engineer, Research and Development Branch, Bureau of Meteorology, Melbourne
and
K. K. WATSON
Associate Professor of Civil Engineering, University of New South Wales

SUMMARY A numerical analysis which is capable of modelling in an unsaturated soil profile any intermittent process involving the application and non-application of water to the soil surface is discussed together with its use in calculating infiltration and surface runoff volumes under varying rainfall intensities. In particular, results are presented for five separate hyetographs each covering a 7-hour period in which the total rainfall remained constant at 150 mm. These results clearly show the sensitivity of infiltration rate and surface runoff to the temporal distribution of rainfall.

## 1 INTRODUCTION

The increasing use in contemporary hydrology of deterministic catchment models to predict surface runoff is resulting in detailed studies becoming necessary in such areas as the spatial nonuniformity of catchment soils and the effect of the temporal variation of rainfall intensity on infiltration behaviour. In this study a numerical rainfall-runoff model is used to investigate the dependence of infiltration and runoff on various time patterns of rainfall intensity. The model is based on a numerical solution of Richards' unsaturated flow equation and is restricted to isothermal, one-phase, vertical flow. Three significant developments in the model are:

(a) a wide variety of initial conditions, boundary conditions and profile characteristics can be handled

(b) the inclusion of a depression storage feature and a switching routine to automatically change the surface boundary condition at the onset and disappearance of surface ponding simulates field conditions and allows for continuing infiltration after the cessation of rainfall

(c) a numerical formulation of the dependent domain model predicts the $h(\theta)$ scanning curves generated during intermittent infiltration-redistribution sequences (Lees and Watson, 1975).

## 2 NUMERICAL ANALYSIS

An earlier paper by Watson and Lees (1975) has demonstrated the ability of the numerical hysteretic rainfall-runoff model to predict, during complicated wetting and drying sequences, the time-dependent relationships of infiltration rate, depression storage and runoff. At this stage, the model cannot be used operationally because of its data requirement and its restriction to one location. However, it is of real current value as a research tool by providing an accurate prediction against which simpler, physically-based approximations can be tested.

The porous material chosen for this study is Rubicon sandy loam. The hydraulic characteristics were presented in Watson and Lees (1975). A homogeneous profile is considered with a low uniform initial water content of 0.164 $mm^3mm^{-3}$. This point lies outside the $h(\theta)$ hysteresis loop and corresponds to a soil water pressure head of -2680 mm of water. The saturated water content is 0.380 $mm^3mm^{-3}$ and the saturated hydraulic conductivity is 0.30 mm $min^{-1}$.

Numerical simulations are conducted with five different hyetographs, identical in all respects except for the input rainfall pattern. In this way different proportions of infiltration and runoff can be related to changes in the rainfall distribution. In each case the total rainfall is 150 mm and the storm duration is seven hours. Except for the constant rainfall intensity case, each intensity is an integral multiple of 0.25 mm $min^{-1}$ and remains constant during each one-hour period. However, the model is not limited in this regard and any time interval or rainfall intensity could have been specified. Hyetographs 1, 2, and 3 shown in Figures 1a, 2a and 3a have the same number of periods of each intensity. The extremes of uniform and highly non-uniform temporal rainfall distributions are represented by including hyetographs 5 and 4 respectively (Figures 5a and 4a).

## 3 DISCUSSION OF RESULTS

In the first hyetograph the most intense rainfall occurs in the initial 60 minute period. During the first three periods the rainfall intensity is 0.75, 0.50 and 0.25 mm $min^{-1}$ respectively. No rainfall occurs during the fourth period. Rainfall is resumed in the fifth period at an intensity of 0.25 mm $min^{-1}$. During the sixth and seventh periods the rainfall intensities are 0.50 and 0.25 mm $min^{-1}$.

The initial rainfall intensity of 0.75 mm $min^{-1}$ is considerably in excess of the saturated hydraulic conductivity. The infiltration rate remains equal to the rainfall intensity for a short time as the surface pressure head value rapidly increases. The surface pressure head is checked at each time step so that the upper boundary condition can be changed to that of surface ponding as soon as the surface pressure becomes zero. This occurs at t = 20 min and immediately the infiltration rate begins to decrease. The depth of water in depression storage increases rapidly as shown in Figure 1c. At t = 55 min the limiting depth of 5.0 mm is reached and runoff begins. The water content profile at t = 60 min is given in Figure 6. By the end of the first period the profile is saturated to -60 mm and the wet front is at -230 mm.

A rainfall intensity of 0.50 mm $min^{-1}$ is imposed at t = 60 min. Because this intensity is greater than the infiltration rate during the period, the depth

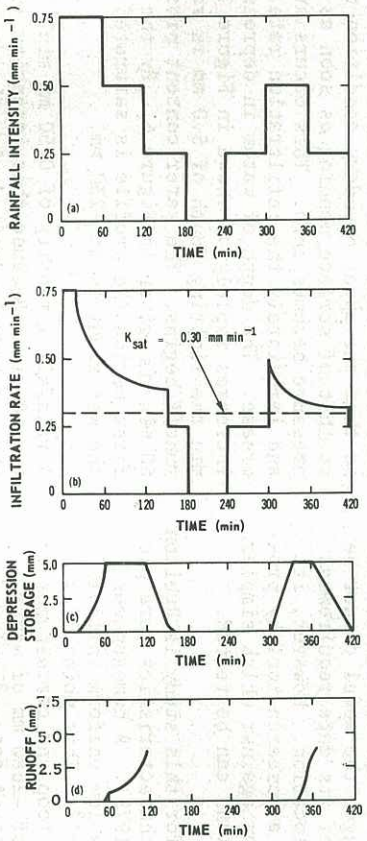


Figure 1

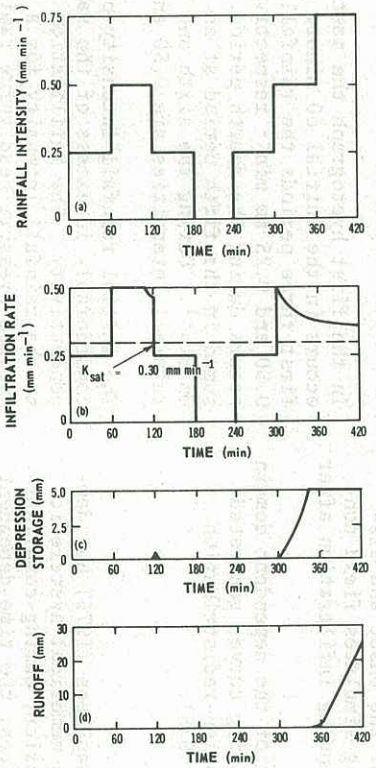


Figure 2

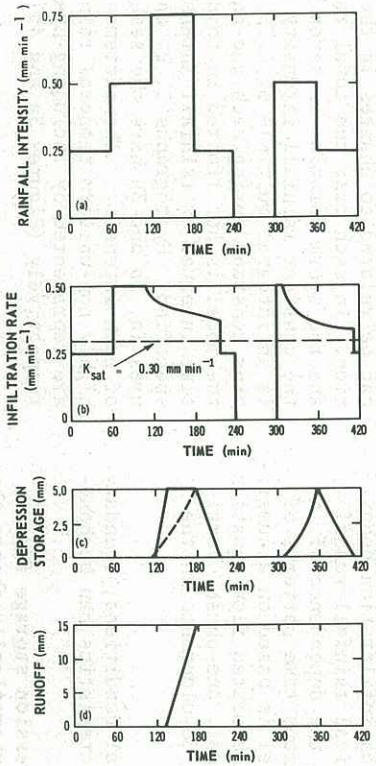


Figure 3

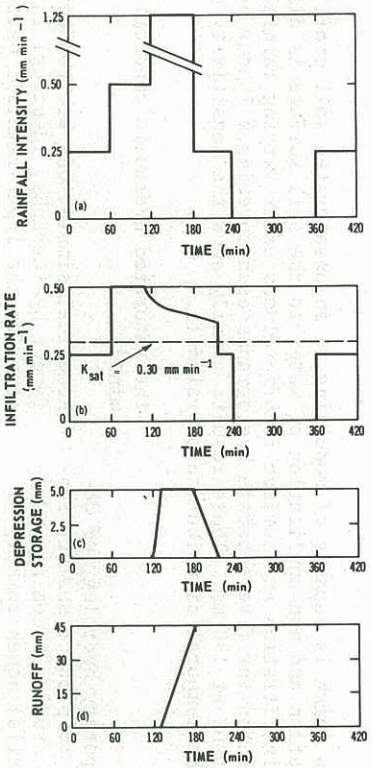


Figure 4

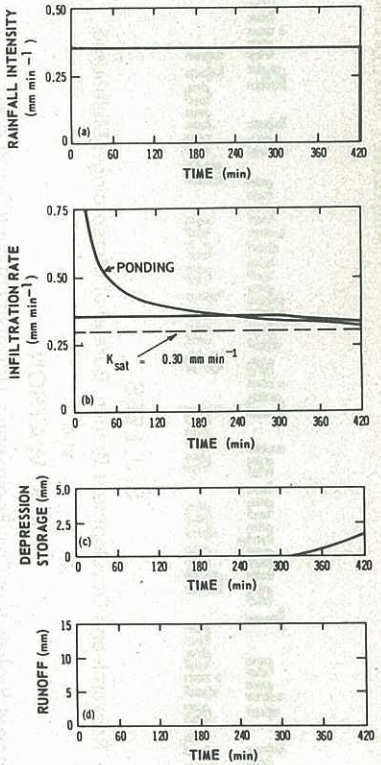


Figure 5

Figures 1-5 Relationships between time and (a) rainfall intensity, (b) infiltration rate, (c) depression storage and (d) runoff. It should be noted that the scales used in representing the runoff are not the same in each figure.

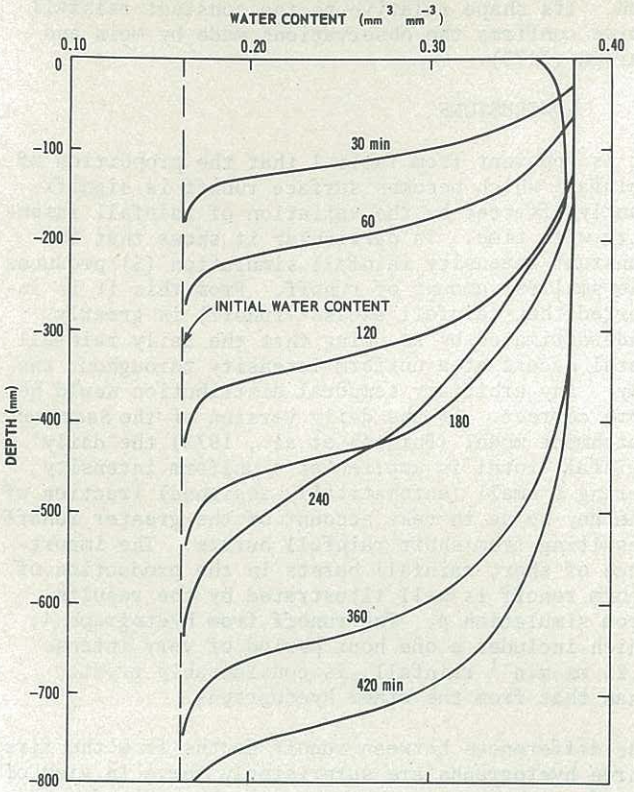


Figure 6 Water content-depth relationships for a profile of Rubicon sandy loam, during infiltration under the rainfall hyetograph shown in Figure 1a

of depression storage remains at the limiting value. The reduction in intensity causes no discontinuity in the infiltration rate, but the runoff rate is noticeably reduced. Runoff continues throughout the second period whilst the infiltration rate decreases. At t = 120 min the saturated zone extends to -120 mm and the cumulative runoff is 3.86 mm.

At the start of the third period the rainfall intensity (0.25 mm $min^{-1}$) is less than the infiltration rate of 0.416 mm $min^{-1}$. Runoff ceases immediately and the water in depression storage begins to dissipate. There is no discontinuity in the infiltration rate curve. The ponded surface boundary condition remains in force until the surface water disappears at t = 155 min, as shown in Figure 1c. The infiltration rate then drops from 0.39 mm $min^{-1}$ to the rainfall intensity of 0.25 mm $min^{-1}$ and remains constant until the end of the period. At t = 180 min pressure reversals have occurred at depths to -230 mm. However, there is no reduction in water content during this period because the draining nodes are described by $h(\theta)$ points on the initial, near-horizontal section of either the boundary draining curve or the primary draining curves.

No rainfall is applied from t = 180 to 240 min. The profile continues to undergo redistribution. Nodes above -230 mm continue along the appropriate draining curve whilst nodes at increasing depths undergo a reversal of pressure and commence to drain. The profile at t = 240 min is given in Figure 6. The profile above -450 mm is draining. The surface has drained past the air entry pressure to -709.4 mm of pressure. The corresponding water content is 0.3608 $mm^3mm^{-3}$. Between z = -450 and z = -680 mm the soil has been wetted by the redistributing water.

At t = 240 min rainfall of intensity 0.25 mm $min^{-1}$ commences and within 4 min pressure reversals have occurred at all draining nodes. The zone from the surface to -120 mm wets up along primary wetting curves which commence at water content values greater than 0.3608 $mm^3mm^{-3}$ and therefore have a very small $d\theta/dh$ gradient. Nodes between z = -120 mm and z = -450 mm follow secondary rewetting curves whilst deeper nodes continue along the boundary wetting curve. The infiltration rate equals the rainfall intensity during this period. The surface pressure at t = 300 min is -111.6 mm, but because of the primary wetting curves being followed the near-surface zone has a water content only slightly less than saturation.

The rainfall intensity is increased to 0.50 mm $min^{-1}$ at t = 300 min. Figure 1b shows that the infiltration rate immediately becomes equal to the rainfall intensity. However the profile is significantly wet by this time. The surface pressure rapidly becomes zero and the infiltration rate begins to drop more quickly than after the previous occurrence of surface ponding at t = 55 min. Correspondingly the rate of depression storage build-up is also greater. The limiting depth is achieved at t = 333 min. Runoff recommences, but at a greater rate than during the second period (when the rainfall intensity was also 0.50 mm $min^{-1}$). The $\theta(z)$ profile at t = 360 min is shown in Figure 6. The upper 320 mm is saturated and the wet front extends to z = -800 mm.

During the final period the rainfall intensity is maintained at 0.25 mm $min^{-1}$. Depression storage depth commences to decrease at t = 360 min; but in this instance 60 min are required for the surface water to dissipate, whereas in the third period (with the same rainfall intensity) only 35 min was required. The free surface water disappears at t = 417 min and the infiltration rate drops to 0.25 mm $min^{-1}$. The pressure reversals during this period are similar to those of the period t = 120 to t = 180 min but extend to -550 mm.

At t = 420 min the wet front has reached -870 mm and the saturated zone extends to -360 mm. During the seven hour period the total rainfall was 150 mm of which 142 mm infiltrated and 8 mm was generated as runoff.

Two further simulations are conducted with hyetographs having the same number of periods of each rainfall intensity as in the first case, but with different time distributions of those intensities. The resultant temporal relationships of rainfall intensity, infiltration rate, depression storage and runoff are shown in Figures 2 and 3. For ease of comparison, the depths of infiltration and runoff, the final wet front and saturated zone depths, and the minimum infiltration rates under surface ponding conditions, from all five simulations, are presented in Table 1.

The hyetograph 4 (see Figure 4a) simulation demonstrates clearly the manner in which relatively short bursts of heavy rainfall produce high rates of surface runoff. During the initial 60 min period surface ponding cannot occur because the rainfall intensity of 0.25 mm $min^{-1}$ is less than the saturated hydraulic conductivity. At t = 60 min the rainfall rate is increased to 0.50 mm $min^{-1}$ and ponding now becomes possible. The surface pressure increases and passes from negative to positive values at t = 111 min. Immediately the upper boundary condition changes. Depression storage commences to build up and the infiltration rate begins to decrease.

The rainfall intensity increases further to 1.25 mm $min^{-1}$ at t = 120 min. During rainfall of this intensity the depression storage fills rapidly. At t = 126 min the storage becomes full and surface runoff commences. Whilst the intense rainfall con-

TABLE 1

RESULTS FROM FIVE RAINFALL-RUNOFF SIMULATIONS IN RUBICON SANDY LOAM

| Hyetograph No. | 1 | 2 | 3 | 4 | 5 |
|---|---|---|---|---|---|
| Cumulative infiltration (mm) | 142.0 | 124.7 | 135.1 | 105.7 | 150.0 |
| Runoff (mm) | 8.0 | 25.3 | 14.9 | 44.3 | - |
| Position of wet front (mm) | -870 | -760 | -830 | -820 | -860 |
| Position of base of saturated zone (mm) | -360 | -260 | -340 | - | -350 |
| Minimum ponding infiltration rate (mm $min^{-1}$) | 0.335 | 0.361 | 0.335 | 0.370 | 0.334 |
| Time of above (min) | 417 | 420 | 413 | 218 | 420 |

tinues runoff takes place at an average rate of 0.74 mm $min^{-1}$, 59% of the rainfall rate. By t = 180 min, 44.3 mm of surface runoff has occurred.

Thereafter the rainfall intensity falls to 0.25 mm $min^{-1}$. The infiltration rate of 0.384 mm $min^{-1}$ is now greater than the rainfall intensity and runoff ceases immediately. The water in depression storage dissipates and, since all subsequent rainfall is less intense than the saturated hydraulic conductivity, no further runoff occurs.

The short time interval rainfall data necessary to detect such rainfall bursts is often unavailable because of the expense of installing and maintaining pluviographs. When using data from a manually-recorded rain gauge it is often necessary to assume that the rainfall has been uniform during the measurement period. The simulation is therefore repeated with the same total amount of rainfall (150 mm) applied at a constant intensity of 0.357 mm $min^{-1}$ throughout the seven hour period. The relative proportions of infiltration and runoff are compared with the proportions resulting from the other non-uniform hyetographs to evaluate the magnitude of any errors caused by an assumption of uniform rainfall intensity.

The rainfall intensity exceeds the saturated hydraulic conductivity of Rubicon sandy loam. The infiltration rate is constant at 0.357 mm $min^{-1}$ until the surface pressure becomes zero at t = 300 min. The subsequent decrease in infiltration rate and increase in depression storage both occur more slowly than in previous simulations. The wetting is monotonic and all nodes follow the boundary wetting curve. At t = 420 min the uppermost 350 mm of the profile is saturated and the wet front is at -860 mm.

The variation of rainfall intensity, infiltration rate, depression storage and runoff with time is shown in Figure 5. The minimum ponded infiltration rate is 0.334 mm $min^{-1}$ and occurs at t = 420 min. The depression storage depth is 1.7 mm at the end of the seven hours. The remaining 148.3 mm has infiltrated into the profile. No runoff has occurred.

The infiltration rate-time curve resulting from infiltration under a small depth (5 mm) of excess surface water is included in Figure 5b for comparison. Its shape relative to the constant rainfall curve confirms the observations made by Mein and Larson (1973).

## 4 CONCLUSIONS

It is apparent from Table 1 that the proportion of rainfall which becomes surface runoff is significantly affected by the variation of rainfall intensity with time. In particular it shows that the constant intensity rainfall simulation (5) produces the smallest amount of runoff. From this it is inferred that rainfall excess (runoff) is greatly underestimated by assuming that the daily rainfall total occurs at a uniform intensity throughout the day. Any arbitrary temporal distribution would be more correct. In the daily version of the Sacramento catchment model (Burnash et al., 1973) the daily rainfall total is applied at a uniform intensity during a small (automatically-assigned) fraction of the day so as to take account of the greater runoff resulting from short rainfall bursts. The importance of short rainfall bursts in the production of storm runoff is well illustrated by the results from simulation 4. The runoff from hyetograph 4, which includes a one hour period of very intense 1.25 mm $min^{-1}$ rainfall, is considerably greater than that from the other hyetographs.

The differences between runoff depths from the first three hyetographs are surprisingly large in view of the fact that these three hyetographs were formed by rearranging a common number of periods of each rainfall intensity. The differences are thus entirely attributable to changes in the temporal distribution. Merely by altering the pattern the runoff-rainfall ratio has increased by a factor of 3.

It is somewhat surprising to note the closeness of the final wet front and saturated zone depths in view of the markedly different infiltration-runoff proportions. The hyetograph 2 depths are somewhat less but this is to be expected because in this case most of the rainfall occurred toward the end of the seven-hour period. Significantly, in this material at least, the constant intensity rainfall simulation provides a reasonable estimate of the final wet front and saturation zone depths. This is important because if a simple means of predicting these depths were found, it might be possible (with judicious assumptions) to apply a model such as the Green and Ampt model to intermittent rainfall conditions.

## 5 REFERENCES


BURNASH, R.J.C., FERRAL, R.L. and McGUIRE, R.A. (1973). A generalized streamflow simulation system. Conceptual modelling for digital computers. U.S. Dept. of Commerce, National Weather Service and State of California, Dept. of Water Resources; Sacramento, Calif., March.

LEES, S.J. and WATSON, K.K. (1975). The use of a dependent domain model of hysteresis in numerical soil water studies. Water Resour. Res., Vol. 11, No. 6, pp. 943-948.

MEIN, R.G. and LARSON, C.L. (1973). Modelling infiltration during a steady rain. Water Resour. Res., Vol. 9, No. 2, pp. 384-394.

WATSON, K.K. and LEES, S.J. (1975). Simulation of the rainfall-runoff process using a hysteretic infiltration-redistribution model. Aust. J. Soil Res., Vol. 13, pp. 133-140.